



## Antimicrobial and toxicity properties of crystalline potassium tetrachlorocuprate (II) dehydrate

M Pavithra & MB Jessie Raj\*

PG and Research Department of Physics, Bishop Heber College,  
Affiliated to Bharathidasan University, Tiruchirappalli-620 017, Tamil Nadu, India

Received 27 February 2021; revised 02 August 2022

In the current scenario, microbial infections are major concern and they multiply so rapidly throughout the world; also, they cause serious bio illness and can even results in death among humans. Complexes framed by crystalline metal ions have been used as medications, because of a wide range of organic activities against harmful microorganisms. In the present study, greenish blue potassium tetrachlorocuprate (II) dihydrate  $K_2CuCl_4 \cdot 2H_2O$  crystalline precipitates were prepared by solvent evaporation method at ambient temperature. This complex was found in nature as a rare mineral Mitscherlichite. For finding the crystalline parameters of the sample, a Single-crystal XRD analysis was used and the data confirms.  $K_2CuCl_4 \cdot 2H_2O$  crystallizes into a tetragonal structure. The formation of bonds and the presence of functional groups in the complex were determined from Surface morphology studies, the very clear morphology of the complex has smoothing surface, defect-free, small microstructures and stacklike shapes of a well-defined crystalline pattern. Also, addition, optical analysis supports that its possibility in antimicrobial applications. The sample shows comparatively good results in positive control of antibacterial and antifungal activities, namely Gentamicin, Chloramphenicol and Clotrimazole.  $IC_{50}$  and optical density (OD) values were used to determine the cytotoxicity and cell viability, respectively. *In vitro* cytotoxicity of MTT assay shows in graphical abstract.

**Keywords:** Mitscherlichite, FT-IR, Microbial control and cell viability, XRD

Developing antimicrobial agents are in tremendous need, play a vital role in biological active applications in therapy and the fast-emerging field of research in this current session. Because bacterial and viral infections spread so quickly, they cause serious bio illness in humans and can even result in death. The systems of microorganisms have various existences. The different types are "bacterials, viruses, fungi, and several organisms". Some illnesses are caused by microorganisms in both direct and unintended ways<sup>1,2</sup>. Strategically, the human death rate in India suggests that most people die due to diseases such as bacterial effects such as cholera, gonorrhoea, bacterial meningitis, and syphilis caused by harmful microorganisms. "The New Diseases of System Effects of the COVID-19" uses antimicrobial activity to solve this cause of infection disease. Researchers recently recorded<sup>3</sup> Nowadays, complexes of metal synthesis growth of crystalline materials have opened a worldwide range of bio applications. By nature, copper-based materials are well-known antimicrobial agents<sup>4</sup>. The impact of microorganisms on human life

began a long time ago and has been different presences, namely, types of microscopic organisms, infections, growth patterns (green growth), and a few on other living beings. Most ailments are legitimately or by implication, brought about by certain sorts of these microorganisms. Deliberately, the investigation of the death rate in India says that a large portion of the individuals are passed on because of microbial infections, we say, cholera, gonorrhoea, bacterial meningitis, and syphilis, brought about by destructive microorganisms<sup>5-6</sup>. This happened because a large portion of the organisms adjusted for anti-infection agents utilised these days<sup>7</sup>. To address these issues, metal particles play an important role in a wide range of widely disparate natural processes, and depending on their location, they may either contribute to the health of the living being or cause harmless<sup>8</sup>. A few metals chelate are known to have antibacterial, fungicidal, antiviral, and anticancer properties. Many metals chelate have been progressively more antimicrobial than the chelating specialist's themselves<sup>9</sup>. Therefore, copper-based mind-boggling compounds were presented, which normally have the tenure to murder microorganisms. During the previous many decades, a tonne of research has

\*Correspondence:  
E-mail: drjessiebhc@gmail.com

worked through specialisation toward medicating disclosure, by considering the least difficult species to contain metal particles and looking into them as the entire compound<sup>10</sup>. The advancement of medication obstruction just as the presence of unfortunate reactions of specific anti-microbials has prompted the hunt for new anti-microbial operators to find new synthetic structures that conquer the symptoms brought about by certain antimicrobial<sup>11-14</sup>. In this work, we report the blend of  $K_2CuCl_4 \cdot 2H_2O$  complex. In this context, as prepared  $K_2CuCl_4 \cdot 2H_2O$  by the combination of potassium chloride (KCL) and copper chloride<sup>15</sup>. A Single Crystal XRD test was undertaken for this copper complex to study the molecular antimicrobial activities were studied by comparing the zone of inhibition against microbes with some antibiotics such as Gentamicin, chloramphenicol, and Clotrimazole arrangements of atoms as well as FT-IR tests were observed to analyse the chemical compound present and bond stretching present in the complex  $K_2CuCl_4 \cdot 2H_2O$  UV-ABS, Transmittance in cytotoxicity<sup>16</sup>. The toxicity level of  $K_2CuCl_4 \cdot 2H_2O$  was understood by calculating the  $IC_{50}$  and OD values. Hereby, we reported the synthesis of  $K_2CuCl_4 \cdot 2H_2O$  and the analysis of their optical properties, FT-IR, antimicrobial, and cytotoxicity activities to the midpoint of future examination to define the finding of new drugs antimicrobial creature. The antimicrobial and cytotoxicity exercises were broken down to arrange future assessments towards the finding of new antimicrobial medications<sup>17-18</sup>. The zone of hindrance against microorganisms was contrasted with a few anti-infection agents, for example, Gentamicin, Chloramphenicol, and Clotrimazole. The harmfulness level of  $K_2 [CuCl_4 \cdot 2H_2O]$  was comprehended by figuring the  $IC_{50}$  and  $OD_{50}$  values.

### Experimental Procedure

The slow evaporation technique is traditionally useful and important. Many crystals are grown by this method, which is utilised for the development of  $K_2CuCl_4 \cdot 2H_2O$  gems at an encompassing room temperature of<sup>19</sup>. Both potassium chloride and sodium chloride are taken in a stoichiometric ratio. Still, as a KCl 15 (mL) dissolved drop solution is applied to distilled water and saturation is achieved,  $CuCl_2$  is applied to dissolve pure water. stirred separately for nearly 30 min in the process of magnetic rousing. To integrate the sample, a stoichiometric proportion of potassium chloride and copper II chloride purchased from Sigma Aldrich is

used. Potassium chloride and, at the same time, copper chloride were separately saturated in deionized water<sup>20</sup>. It is homogeneously mixed by using a magnetic stirrer until the supersaturation is acquired. To maintain homogeneous blending, potassium chloride solution was gradually added drop by drop to the copper chloride solution. The solution was filtered using Whatman channel paper.

The filtered green-coloured supersaturated solution was kept aside for moderate dissipation. The experimental procedure for preparing the solution to get  $K_2CuCl_4 \cdot 2H_2O$ <sup>21</sup>. Crystal is pictorially represented in (Fig. 1). For nearly a month, the well-known greenish-blue colour copper complex of potassium tetrachlorocuprate (II) dihydrate has been grown, as shown in (Fig. 2).

### Antimicrobial Process

The antimicrobial activity microorganism applications on copper surfaces were considered as well-prepared using  $K_2CuCl_4 \cdot 2H_2O$  to crystalline. The example was tried against bacterial four pathogenic bacteria strains including two methods of Gram-positive and Gram-negative life forms and one organism *Candida* cause of infection [Immunity of *Bacillus* sp., *Staphylococcus aureus*, and *Candida* sp.] were arranged exclusively in Nutrient agar and (SDA) medium and saved a vaccine, *Escherichia coli*, *Pseudomonas* sp for brooding at the appropriate temperature. The bacterial inoculum was uniformly spread using a sterile cotton swab on a sterile Petri dish containing nutrient agar media. After inoculation,

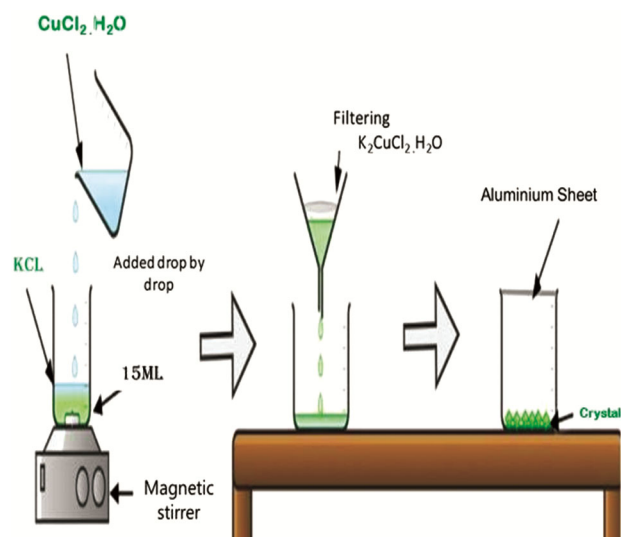


Fig. 1 — Schematic representation of Synthesis Procedure of  $K_2CuCl_4 \cdot 2H_2O$  crystals

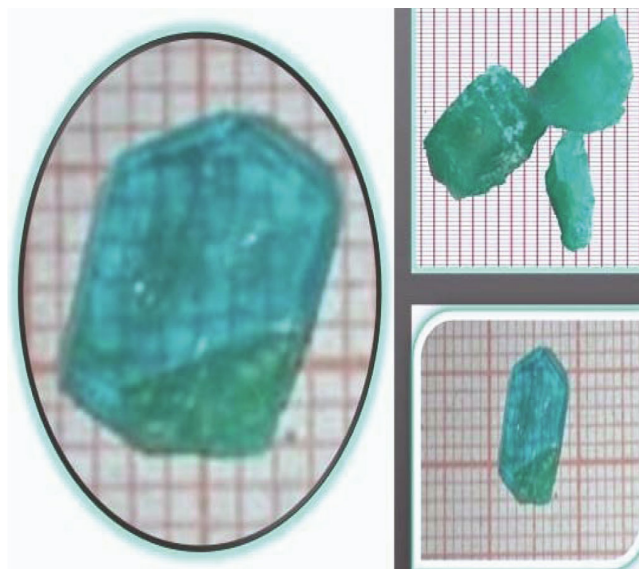


Fig. 2 — Grown Greenish blue Potassium tetrachlorocuprate (II) dehydrate crystals

well loaded with test samples. Then plates were incubated at (37°C for 24 h) using crystals of the zone of inhibition was measured using a zone reader. The method of Muller-Hinton is plated were clean (cotton buds) the hold 8 h the culture of stock it separates of microorganisms of pathogenic. Vaccination effect at a size of 10 nm in width and around two centimetres, as a section of each plate utilizing sterile plug borer. The various range from 100 L, the dissolvable medication dose of medication dissolvable. Growth of bacterial and fungal at room temperature within 3 days.

#### Composition of Muller Hinton Agar Media

Beef Extract (02.00 g/Lit), Acid Hydrolysate of Casein, (17.50 g/Lit), Starch (01.50 g/Lit), Agar (17.00 g/Lit) the various composition Agar Media.

#### MTT assay for cell cytotoxicity

The assay MTT explain is (3-4, 5 dimethylthiazol-2-yl-2,5-diphenyl tetrazolium bromide) assay, the systematic at the ability based on cells of Mitochondrial dehydrogenase enzyme is the membrane of cell visible the clave the rings of tetrazolium, it is pale-coloured yellow and MTT from dissolved crystals of dark blue colouring crystals formed using formazan, which is Largely impermeable assay based onto cell membranes, thus resulting in its accumulation within healthy cells. Solubilisation of cells by the addition of detergents 1 mL added in dimethyl sulfoxide (DMSO) results in

Table 1 — Single-crystal XRD data of the  $K_2CuCl_4 \cdot 2H_2O$  crystal

Comparative result	Unit cell dimension						Cell volume ( $\text{\AA}^3$ )
	a ( $\text{\AA}$ )	b ( $\text{\AA}$ )	c ( $\text{\AA}$ )	$\alpha$ ( $^\circ$ )	$\beta$ ( $^\circ$ )	$\gamma$ ( $^\circ$ )	
Values from literature	7.45	7.45	7.88	90	90	90	437.4
Obtained values	7.459	7.459	7.830	90	90	90	435.8

the liberation of crystals which are solubilized. The more numbers of surviving cells are proportional directly. The crystal created the Formazan, the very quantified of a reader multi-Well plate. DMEM medium, fetal Bovine Serum (FBS) and antibiotic medicine used were from Gibco (USA), we have the formation of DMSO (Dimethyl sulfoxide) and MTT (3-4,5 dimethylthiazol-2-yl-2,5-diphenyl-tetrazolium bromide) using the (5 mg/mL) were from (USA) Sigma, 1X PBS was from Himedia, (India). 96 well tissue culture plate and wash conical beaker were from Tarson (India).

## Results and Discussion

#### Single-crystal x-ray diffraction analysis

Important of X-ray diffraction is the Single-crystal effect of analysis. The Potassium tetrachlorocuprate (II) dihydrate crystal was carried out using Bruker APEX II single crystal diffractometer with  $CuK\alpha$  radiation ( $\lambda=0.71073\text{\AA}$ )<sup>22</sup>. Carefully cut crystals of (0.2 × 0.3 × 0.6 mm) are used to measure the cell parameters and cell volume. Unit cell dimensions,  $a = b \neq c$ , and  $\alpha = \beta = \gamma$  and which confirms the complex is tetragonal structured crystal<sup>23</sup>. The determining unit cell parameter was used to find the volume and tabulated in (Table 1).

#### FTIR analysis

The FT-IR of  $K_2CuCl_4 \cdot 2H_2O$  was recorded by the wavenumber ranges from  $400\text{cm}^{-1}$  to  $4000\text{cm}^{-1}$  using the Perkin Elmer spectrometer by KBr pellet technique. Spectroscopy is a powerful instrument for verifying the characteristic of the chemical bond located in the molecules by absorbing the wavelength of the light such as the infrared absorption spectrum. FT-IR spectra of  $K_2CuCl_4 \cdot 2H_2O$  shown in (Fig. 3). The band range of  $3500\text{cm}^{-1}$  and  $3000\text{cm}^{-1}$  shows the presence of high Potassium chloride concentration. The characteristic vibration of O-Presence stretching found at  $3378\text{cm}^{-1}$  infrared absorption spectra<sup>25</sup>. The characteristic FT-IR spectra of  $K_2CuCl_4 \cdot 2H_2O$  are shown in (Fig. 3) The band

range of ( $3500\text{ cm}^{-1}$  and  $3000\text{ cm}^{-1}$ ) shows the presence of high Potassium chloride concentration<sup>24</sup>. The characteristic vibration of O-HC presence stretching. We have found at  $3378\text{ cm}^{-1}$ . This next stretching vibration of peaks point at ( $1519\text{ cm}^{-1}$  and  $1403\text{ cm}^{-1}$ ) may overlay the diagnostic bands of Cu-based pigments<sup>25</sup>. OH, the bending peaks absorbed between ( $1049\text{ cm}^{-1}$  and  $1021\text{ cm}^{-1}$ ). this some wavenumber appeared midpoint at ( $932\text{ cm}^{-1}$  and  $867\text{ cm}^{-1}$ ), the peak designated as the O-Cl compound ion as stretching vibrations. The peaks ion as stretching vibrations. The peaks absorbed between ( $558\text{ cm}^{-1}$  range to  $430\text{ cm}^{-1}$ ) are the vibration of stretching due to inspection of halides (Chloride) with

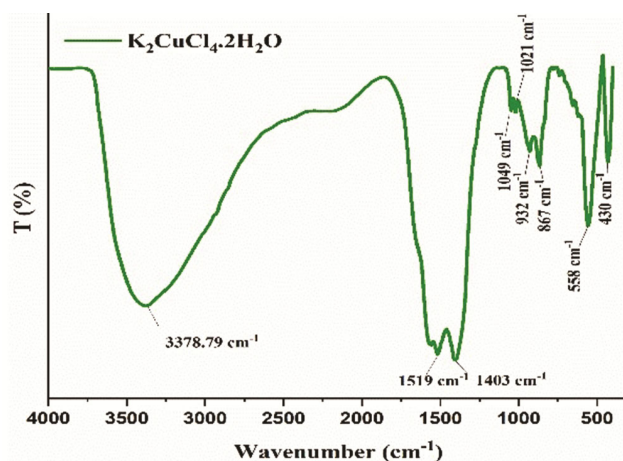


Fig. 3 — FT-IR spectrum of  $\text{K}_2\text{CuCl}_4 \cdot 2\text{H}_2\text{O}$  crystal

K/Cu. The slight shift in the frequency of vibrations may be due to dopant concentration in the crystal growth<sup>26</sup>.

#### Optical properties

The absorption spectrum of  $\text{K}_2\text{CuCl}_4 \cdot 2\text{H}_2\text{O}$  is monitored between 300 and 800 nm. Even though the crystal is bluish green, it is more transparent in the visible region shown in (Fig. 4A). Peaks centered between 370 and 507 nm. From the result, it is evaluated that the crystal can be used for green-emitting LED's light with good optical properties and applied microbial activity<sup>27</sup>. Similarly, the transmittance of UV is the spectrum obtained between the range of 300 nm and 800 nm. (Fig. 4B) This cut-off wavelength is well agreed upon. Interestingly, the entire range visible point region at (371-800 nm), the maximum of transmittance is acquired at (371 nm to 509 nm) the intensity of transmission light decreased with the increase of thickness of the medium<sup>28</sup>. The crystals have almost negligible absorption. The significant valley peak near 800 nm, which corresponds to infrared, may be enhanced application in antimicrobial applications. It reveals that the samples have strong. The transmittance decreases after increasing  $\text{K}_2\text{CuCl}_4 \cdot 2\text{H}_2\text{O}$ . The dependence upon the coefficient of optical energy and absorption, with the help of energy photons due to the various structures and defined ions in compound band structures and the many types of modern tech

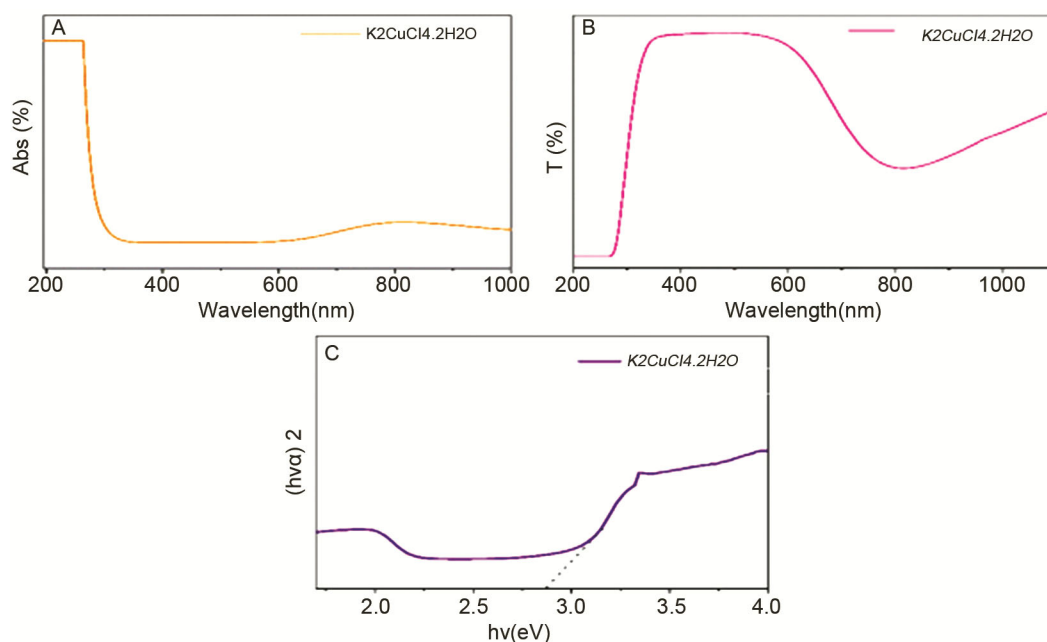


Fig. 4 — (A) Absorption; (B) transmission; and (C) Energy band gap spectra of  $\text{K}_2\text{CuCl}_4 \cdot 2\text{H}_2\text{O}$  Crystal

transitions of electrons<sup>29</sup>. The graph was a plot between  $(h\nu\alpha)^2$  and energy  $(h\nu)$  eV. From the graph shown (Fig. 4C) energy band gap, this indicates that the sample shows the plot of the variation of photon energy in the linear region of the curve was extra plotted to find the X intercept which gives the energy band gap defined the grown crystalline, Therefore, the energy band gap of  $K_2CuCl_4 \cdot 2H_2O$  was determined as 2.85 eV.

#### Surface Morphology

The surface morphology of the crystals was evaluated by collecting top-view images using a scanning electron microscope (SEM)<sup>30</sup>. SEM image was taken as 6.07 kx magnification with an acceleration voltage of (10 kV). It is observed that many microstructural crystallites were seen on the surface of the crystalline  $K_2CuCl_4 \cdot 2H_2O$  and have lesser defects<sup>31</sup>. The surface has well defined stacking layers with periodic form. A homogeneous distribution with some uniform pattern formed on some clear shape of quartz surface of the crystal grown and is propagated along with morphology like a surface plane shows that (Fig. 5) surface morphology.

#### Dielectric Studies

The analysis using the important studies, and belonging, the effect of the dielectric can use parameters such as two types of dielectric constant and loss are the basic electrical properties of solids. The measurement of dielectric constant and loss as a function of the frequency of room temperature gives

many ideas of electrical procedures that are occurring in material and Mixes,  $K_2CuCl_4 \cdot 2H_2O$ <sup>32</sup>. Single crystal is subjected to the measurement of dielectric<sup>33</sup>. Constant and loss as a function of frequency from (50 Hz to 2 kHz). Dielectric constant and dielectric loss measurement as a function of the frequency at room temperature gives idea on electrical procedures that are occurring in material.

$K_2CuCl_4 \cdot 2H_2O$  single crystal is subjected to the measurement of dielectric constant and loss as a function of frequency from (50 Hz to 2 kHz). Figure 6A & B shows that (A) dielectric constant (B) dielectric loss of the  $K_2CuCl_4 \cdot 2H_2O$  is normal and resonance dielectric behaviour. Dielectric constant and dielectric loss decrease with increasing frequency and attains saturation at higher frequencies. The important vital role of four polarization parameters namely space charge, orientation, frequency. The high values of dielectric constant and dielectric loss at lower frequencies are ascribed to space charge polarization. In the same way, low values of dielectric constant and dielectric loss at higher frequencies reveal the grown crystal with good optical quality and lesser defects. The recorded dielectric study reveals the defect-free crystallinity nature of  $K_2CuCl_4 \cdot 2H_2O$  prevalent extremely significant for antimicrobial applications.

#### Antimicrobial activities

Harmful microbes are becoming more tolerant to most of the antibiotics, some complex materials are

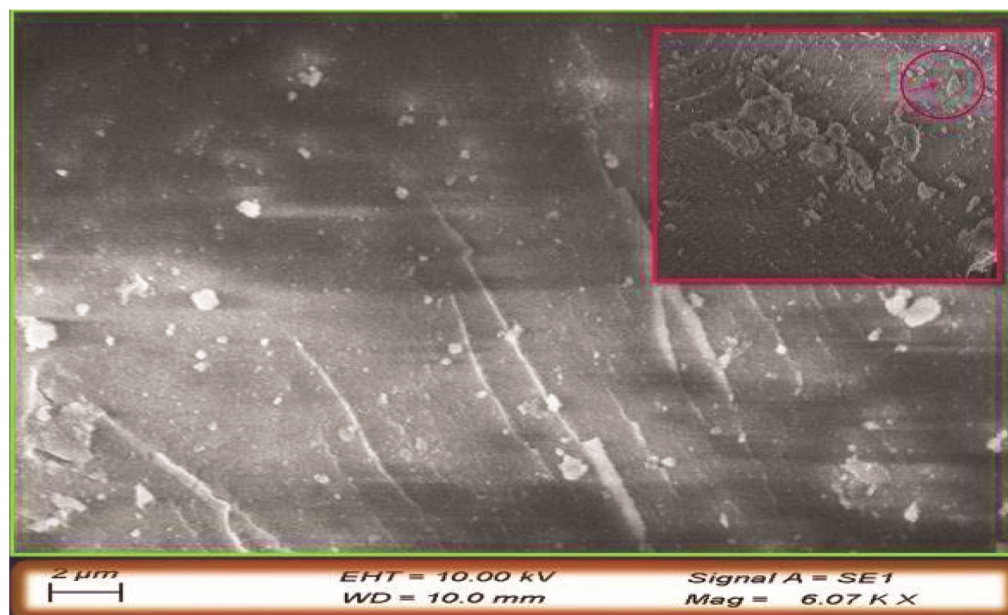


Fig. 5 — Surface Morphology of  $K_2CuCl_4 \cdot 2H_2O$  crystal

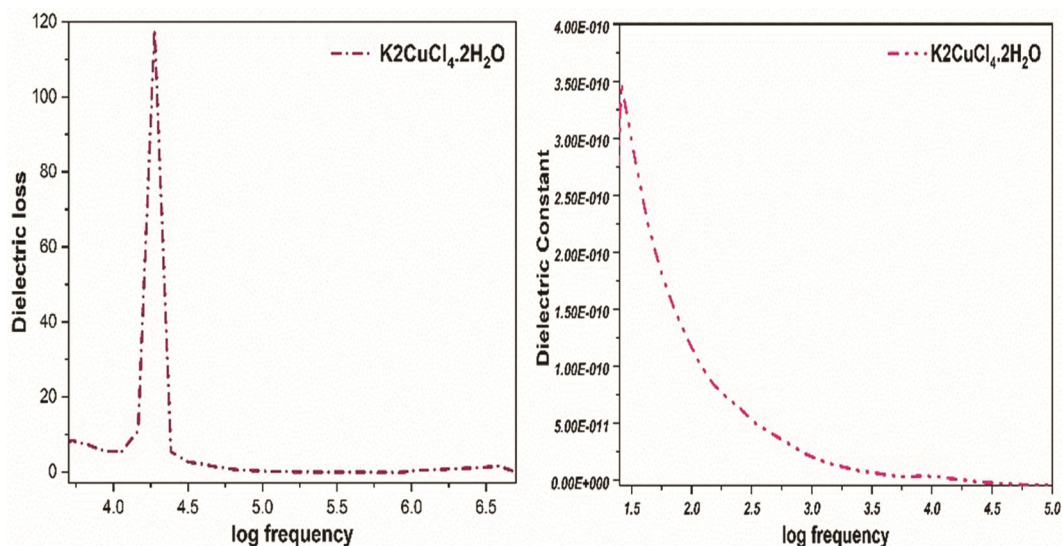


Fig.6 — The Dielectric studies responses, (A) Dielectric loss, and (B) Dielectric constant of function of frequency

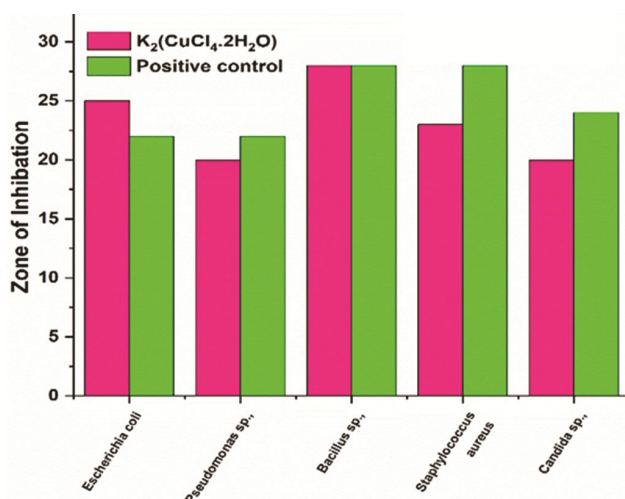


Fig. 7 — Comparative chart of  $K_2CuCl_4 \cdot 2H_2O$  against pathogens

introduced to kill harmful microbes. In this study Potassium tetrachlorocuprate (II) dihydrate is used to study the antimicrobial activities against various microbes<sup>34</sup>. The Antimicrobial activity of Sample  $K_2CuCl_4 \cdot 2H_2O$  has exposed that good antimicrobial activity against tested pathogens. In this experiment, the anti-microbial activity of the samples we show that testing zone of Inhibition of the microbial activity of (ZOI) microbial assay. Few fast decays, after incubation, Effect of zone production on this, plates were read as per the defined standard well know Zone of Inhibition (ZOI) Anti-microbial assay shows that (Fig. 7) zone o inhibition of the sample correlated with positive control and  $K_2CuCl_4 \cdot 2H_2O$  different activity. the explain of the Antimicrobial Activities of Various Samples by Agar Well Diffusion Method of

test sample  $K_2CuCl_4 \cdot 2H_2O$  Table (2) the shows that (Fig. 8) the different types of pathogens represent the zone of inhibition of the complex, test sample  $K_2CuCl_4 \cdot 2H_2O$  against microbes the correlated with the result of positive controls such as Gentamicin, Chloramphenicol, and Clotrimazole<sup>35</sup>. From this result,  $K_2CuCl_4 \cdot 2H_2O$  shows that. More sensitivity against (*Escherichia coli* and *Bacillus sp.*), and good antibacterial activities. This verifies that the complex has the Tendency to act as an antibiotic solution. The zone of kill the antimicrobial.

#### Cytotoxicity analysis

The cytotoxicity of the  $K_2CuCl_4 \cdot 2H_2O$  is tested in which cell toxic inspect of the vitro and cells of Vero, culture by the “3-(4, 5-dimethylthiazol-2-yl) 2, 5” diphenyltetrazolium bromide assay (MTT). Vero cell cluster, (African green monkey tested cells), cluster cell line was purchased. Using ten percent of liquid medium (DMEM), supplemented ten percent (FBS), each of 100  $\mu\text{g}/\text{mL}$  used the penicillin and streptomycin, cells were cultured and kept at the atmosphere of five percent ( $\text{CO}_2$  at  $37^\circ\text{C}$ ). [47] Briefly, by trypsinization, cultured Vero cells were collected in a 15 mL tube<sup>36</sup>. Then, a density of  $1 \times 10^5$  cells/mL cells/well (200  $\mu\text{L}$ ) cells were plated into a 96- well tissue culture plate DMEM medium containing (10 %) FBS & (1%) antibiotic solution for (24-48 h at  $37^\circ\text{C}$ ). Sterile PBS was used to wash wells the variation of samples of different concentrations tested with free-serum and medium of DMEM. the sampled done of three trials was cells were incubation of Humidified five percent  $\text{CO}_2$  used incubator initials

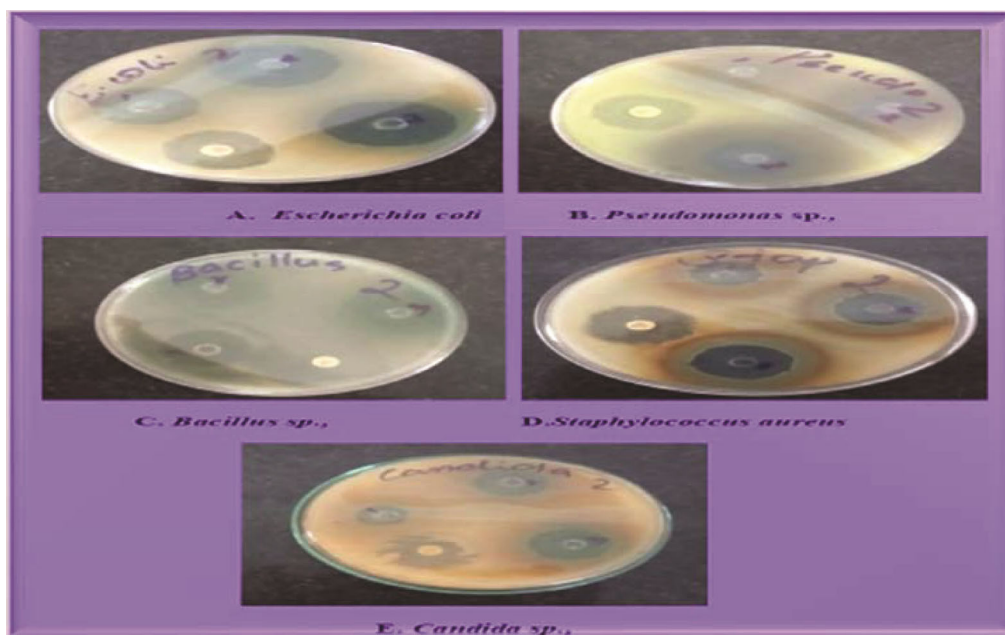


Fig. 8 — Zone of inhibition of the sample  $K_2CuCl_4 \cdot 2H_2O$  against Microbes

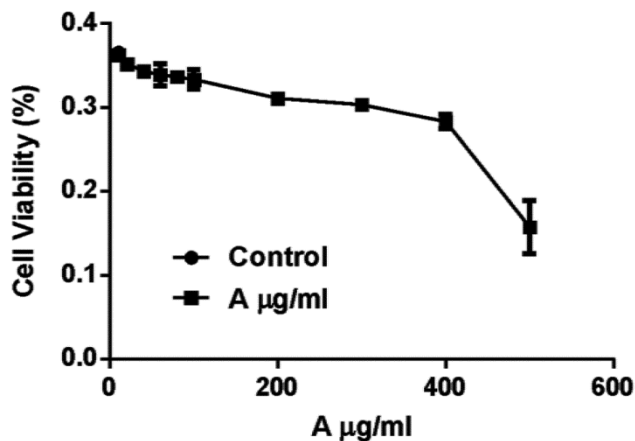


Fig. 9 — Cell Viability of  $K_2CuCl_4 \cdot 2H_2O$  crystal

degree of (37°C of 24 h). Used MTT assay was using the added (20 µL & 5 mg/mL) after the incubation particular period<sup>37</sup> into each well and until the precipitate of purple colour, were visible under an inverted microscope of under visible source. The cells were incubated for another (2-4 h). Finally, the medium together with 220 (µL) of MTT was aspirated off the wells and using (200 µL) of 1X PBS washed. For dissolving formazan crystals, DMSO 100 (µL) was added and the plate was agitated for five minutes. each well was noted at the absorbance of 570 nm using a microplate reader, the cell viability percentage of the deliberate IC<sub>50</sub> value was calculated using Graph pad is plot using software, As the result, these

Table 2 — Antimicrobial Activities by Agar Well Diffusion Method

S. No	Pathogens	Zone of Inhibition (mm)	Control value
1	<i>Escherichia coli</i>	Gentamicin 22 mm	Sensitive 25 mm
2	<i>Pseudomonas sp.</i> ,	Chloramphenicol 22 mm	Sensitive 20 mm
3	<i>Bacillus sp.</i> ,	Chloramphenicol 28 mm	Sensitive 28 mm
4	<i>Staphylococcus aureus</i>	Chloramphenicol 28 mm	Sensitive 23 mm
5	<i>Candida sp.</i> ,	Clotrimazole 24 mm	Sensitive 23 mm

compound shows higher toxicity to a higher concentration and lower toxicity to minimum concentration<sup>38</sup>. The cell viability of the control of prepared cell shows that (Fig. 9). Table 3 shows the sample concentration of optical density of crystal treated cell various types of mean value. The cytotoxicity of the  $K_2CuCl_4 \cdot 2H_2O$ .

**Percentage of Cell Viability**

The cell lines were exposed, material complexes are used at various concentrations of different ranges of (10 to 500 µg/mL for 24 h). Therefore, Results found that indicated a selective effect of the copper complexes in favour of Vero cells. The doses lower than 200 µg/mL, no significant decrease in cell viability was observed Table 4 Percentage of Cytotoxicity of  $K_2CuCl_4 \cdot 2H_2O$  with various concentration of optical density value 570 nm and

Table 3 Optical Density (OD) values of treated cells

S. No	Sample concentration	OD Values at 570 nm		
1	Control	0.372	0.361	0.363
2	10 µg/mL	0.359	0.362	0.365
3	20 µg/mL	0.355	0.362	0.365
4	40 µg/mL	0.348	0.342	0.339
5	60 µg/mL	0.340	0.325	0.351
6	80 µg/mL	0.331	0.333	0.345
7	100 µg/mL	0.328	0.346	0.325
8	200 µg/mL	0.313	0.306	0.312
9	300 µg/mL	0.299	0.30	0.281
10	400 µg/mL	0.276	0.292	0.281
11	500 µg/mL	0.121	0.179	0.171

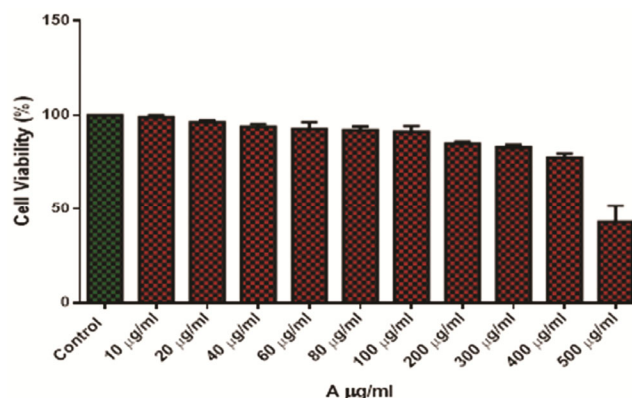
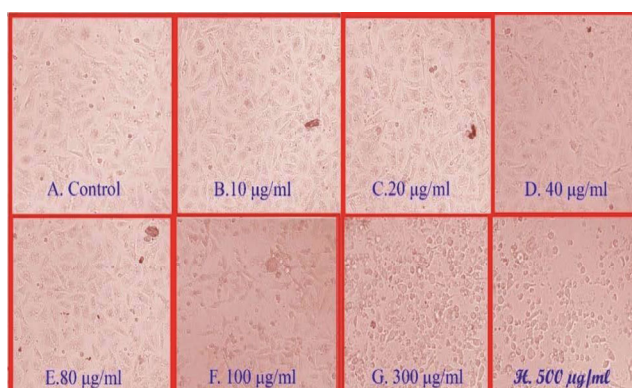
Table 4 — Cytotoxicity of  $K_2CuCl_4 \cdot 2H_2O$  at optical density value 570 nm

S. No	Tested Sample concentration (µg/mL)	OD values at 570 nm (in triplicates)			
1	Control	100	100	100	100
2	10 µg/mL	98.35	99.17	100	99.17
3	20 µg/mL	97.26	95.06	96.43	96.25
4	40 µg/mL	95.34	93.69	93.98	93.98
5	60 µg/mL	93.15	89.04	96.16	92.78
6	80 µg/mL	90.68	91.23	94.52	92.14
7	100 µg/mL	89.86	94.79	89.09	91.21
8	200 µg/mL	85.75	83.83	89.547	86.40
9	300 µg/mL	81.91	84.65	82.46	82.85
10	400 µg/mL	75.61	76.98	77.53	
11	500 µg/mL	33.15	49.4	46.84	43.13

mean value. At the doses of (300 and 500 µg/mL), cell viability lowered to 82.85 and 43.13%. Under cell viability data, the copper complexes were determined to be more effective.  $IC_{50}$  Value of tested sample is found to be 364.1 µg/mL. As to the morphological observations of shows that (Fig. 10) graphical representation of control cells and  $K_2CuCl_4 \cdot 2H_2O$  of different cell viability of treated cell. there was mild to moderate degeneration on the cells at the dose of 300 µg/mL copper (II) complex. However, the cells almost lost their characteristic morphology and became rounded and shrunken at the dose of (500 µg/mL) copper (II) complex (Fig. 11). The inverted microscopic image of controlled and (10-500 µg/mL).  $K_2CuCl_4 \cdot 2H_2O$  treated cells Besides, the number of cells reduced considerably. In our study shows that Percentage of Cytotoxicity of  $K_2CuCl_4 \cdot 2H_2O$  with various concentration of optical density value 570nm and mean value (Table 4).

### Conclusion

Potassium tetrachlorocuprate (II) dihydrate  $K_2CuCl_4 \cdot 2H_2O$  were prepared by slow evaporation

Fig. 10 — Graphical representation of  $K_2CuCl_4 \cdot 2H_2O$  against cell viability of treated cellsFig. 11 — Inverted microscope images of treated cells by  $K_2CuCl_4 \cdot 2H_2O$ 

method with the development of greenish-blue precious stone. From single-crystal XRD analysis, it is seen that  $K_2CuCl_4 \cdot 2H_2O$  is a tetragonal structure. FT-IR spectra confirmed that the arrangement of  $K_2CuCl_4 \cdot 2H_2O$  and their bond formation. UV transmittance and calculated energy band gap of the crystal shows the applicability of the sample in antimicrobial applications. The dielectric properties are well known that exposed the application of studies. The surface morphology studies showed defect less good crystalline structure. The antimicrobial activities of  $K_2CuCl_4 \cdot 2H_2O$  show the crystals can use as antibiotics. To realize its toxicity level, cytotoxicity examinations were made.  $IC_{50}$  Value of  $K_2CuCl_4 \cdot 2H_2O$  is found to be 364.1 µg/mL. The result uncovered that  $K_2CuCl_4 \cdot 2H_2O$  has less toxicity. There are numerous chances in curing Vero cells, future examinations ought to be progressively cantered around this region. At last, we presume that  $K_2CuCl_4 \cdot 2H_2O$  tend to use as anti-infection agents, this research may invigorate perusers to discover novel applications in therapy.

## Acknowledgement

This characterisation work has been supported by sophisticated Analytical and instruments facility (SAIF) sophisticated Test and instrumentation centre cochin university Campus, Kerala. Fourier Transform Infrared Spectrometer at the department of instrumentations. Joseph College, Trichy.

## Conflict of interest

All authors declare no conflict of interest.

## References

- Bashir F, Irfan M, Ahmad T, Iqbal J, Butt MT, Sadeq Y, Umbreen M, Sheikh IA & Moniruzzaman M, Efficient utilization of low-cost agro materials for the incorporation of copper nanoparticles to scrutinize their antibacterial properties in drinking water, *Environ Technol Innov*, (2020) 101228.
- Morens D & Fauci AS, Emerging Pandemic Diseases: How we got to COVID-19. *Cell*, 182 (2020) 1077.
- Konduri VV, Kalagatur NK, Nagaraj A, Kalagadda VR, Mangamuri UK, Durthi CP & Poda S, *Hibiscus tiliaceus* mediated phytochemical reduction of zinc oxide nanoparticles and demonstration of their antibacterial, anticancer, and dye degradation capabilities. *Indian J Biochem Biophys*, 59 (2022) 565.
- Han D, Yan Y, Bian X, Wang J, Zhao M, Duan X & Ding S, A novel electrochemical biosensor based on peptidoglycan and platinum-nickel-copper nano-cube for rapid detection of Gram-positive bacteria. *Microchemical Acta*, 187 (2020) 607.
- Liu T, Application of IoT image detection and DWI combined with serum PCT detection in bone infection. *Microprocess Microsyst*, 81 (2021) 103665.
- Kumar A, Zhang y, Liu W & Sun X, The chemistry, recent advancements and activity descriptors for macrocycles based electrocatalysts in oxygen reduction reaction. *Coordinat Chem Rev*, 402 (2020) 213047.
- Zhou J, Xu X, Duan B, Wu H, Shi J, Luo Y & Meng Q, Regulating crystal growth via organic lithium salt additive for efficient Kesterite solar cells. *Nano Energy*, 89 (2021) 89.
- Azizi-Lalabadi M, Hashemi H, Feng J & Jafari S, Carbon nanomaterials against pathogens; the antimicrobial activity of carbon nanotubes, graphene/graphene oxide, fullerenes, and their nanocomposites. *Adv Colloid Interface Sci*, 184 (2020) 102250.
- Jin X, Xiao Q, Xu T, Huang G, Wu H, Wang D, Liu Y, Zhang H & Lai, Thermal conductivity enhancement of a sodium acetate trihydrate–potassium chloride–urea/expanded graphite composite phase–change material for latent heat thermal energy storage. *Energy Build*, 231 (2021) 110615.
- Núñez-González R, Aceves R, Cabellos J & Posada-Amarillas A, Effect of Substitutional Cu atoms on the Electronic and Optical Properties of KCl: A DFT Approach. *Mater Today Commun*, (2019)100831.
- Siqwepu O, Salie K & Goosen N, Evaluation of potassium diformate and potassium chloride in the diet of the African catfish, *Clarias gariepinus* in a recirculating aquaculture system. *Aquaculture*, 526 (2020) 735414.
- Bodryakov, Joint Analysis of the Heat Capacity and Thermal Expansion of Solid Potassium Chloride. *Inorg Mater*, 56 (2020) 633.
- Singh S, Numan A, Somaily H, Gorain B, Ranjan S, Rilla K, Siddique HR & Kesharwani, Nano-enabled strategies to combat methicillin-resistant *Staphylococcus aureus*. *Mater Sci Eng: C*, 129 (2021) 112384.
- Kumar NS & Rayar SL, Synthesis, crystal growth and characterization of semi-organic NLO materials: L-valine copper chloride as optoelectronic sensor. *Indian J Phys*, 96 (2022) 79.
- Suzuki A, Kitagawa K, Oku T, Masanobu Okita, Fukunishi S & Tachikawa T, Additive Effects of Copper and Alkali Metal Halides into Methylammonium Lead Iodide Perovskite Solar Cells. *Electron Mater Lett*, 18 (2022) 176.
- Kiriukhina GV, Yakubovich OV, Dimitrova OV & Volkov AS, New Microporous Copper Diphosphate Chloride in a Series of Homeotypic Compounds: Hydrothermal Synthesis, Crystal Structure, and Crystal Chemistry. *Crystallogr Rep*, 67 (2022) 545.
- Hui-Min R, Hong-Wei W, Yuan-Fan J, Zhi-Xiong T, Chen-Yu M & Li G, Proton Conductive Lanthanide-Based Metal–Organic Frameworks: Synthesis Strategies, Structural Features, and Recent Progress. *Top Curr Chem (Z)*, 380 (2022) 9.
- Cobos m, De-La-Pinta I, Quindós G, Fernández M & Fernández M, Synthesis, physical, mechanical and antibacterial properties of Nanocomposites based on poly (vinyl alcohol)/Graphene oxide–silver nanoparticles. *Polymers*, 12 (2020) 723.
- Meenatchi V, Siva S & Cheng L, Synthesis, crystal growth, spectroscopic characterization, Hirshfeld surface analysis and DFT investigations of novel nonlinear optically active 4-benzoylpyridine-derived hydrazone. *J Mol Struct*, 1243 (2021) 130858.
- Qian W, Xu X, Wang J, Xu Y, Chen J, Ge Y, Chen J, Xiao S & Yang, An aerosol-liquid-solid process for the general synthesis of halide perovskite thick films for direct-conversion X-ray detectors. *Matter*, 4 (2021) 942.
- Rajkumar R & Kumar PP, Structure, crystal growth and characterization of piperazinium bis(4-nitrobenzoate) dihydrate crystal for nonlinear optics and optical limiting applications. *J Mol Struct*, 1179 (2019) 108.
- Gao W, Yin L, Yuan JH, Xue KH, Niu G, Yang B, Hu Q, Liu X & Tang J, Lead-free violet-emitting K<sub>2</sub>CuCl<sub>3</sub> single crystal with high photoluminescence quantum yield. *Org Electron*, 86 (2020) 105903.
- Jin X, Xiao Q, Xu T, Huang G, Wu H, Wang D, Liu Y, Zhang H & Lai, Thermal conductivity enhancement of a sodium acetate trihydrate–potassium chloride–urea/expanded graphite composite phase–change material for latent heat thermal energy storage. *Energy Build*, 231 (2021) 110615.
- Balakrishnan S, Duraisamy S, Kasi M, Kandasamy S, Sarkar R & Kumarasamy A, Syntheses, physicochemical characterization, antibacterial studies on potassium morpholine dithiocarbamate nickel (II), copper (II) metal complexes and their ligands. *Heliyon*, 5 (2019) e01687.
- Vijayalakshmi M, Ravindran B & Anitha M, Growth and characterization of succinic acid potassium chloride mixed crystals. *Mater Today: Proc*, 46 (2021) 3915.

- 26 Krishnamoorthi R & Uvarani G, Growth and characterization of pure and metals-doped organic nonlinear optical single crystal: L-alanine alaninium nitrate (LAAN). *J Mater Sci: Mater Electron*, 32 (2021) 3979.
- 27 Johnson J, Srinivasan R & Sivavishnu D, In depth study on growth aspects and characteristic properties of semiorganic nonlinear optical crystal: 4-Dimethylaminopyridine copper chloride. *Mater Sci Energy Technol*, 2 (2019) 226.
- 28 Ali HE & Khairy Y, Optical and electrical performance of copper chloride doped polyvinyl alcohol for optical limiter and polymeric varistor devices. *Physica B: Condensed Matter*, 572 (2019) 256.
- 29 Kumar NS & Rayar SL, Synthesis, crystal growth and characterization of semi-organic NLO materials: L-valine copper chloride as optoelectronic sensor. *Indian J Phys*, 96 (2022) 79.
- 30 Chen X, Wei S, Wang Q, Tang M, Shen X, Zou X, Shen Y & Ma B, Morphology Prediction of Portlandite: Atomistic Simulations and Experimental Research. *Appl Surf Sci*, (2019) 144296.
- 31 Alesary HF, Ismail HK, Odda AH, Watkins MJ, Majhool AA, Ballantyne AD & Ryder KS, Influence of different concentrations of nicotinic acid on the electrochemical fabrication of copper film from an ionic liquid based on the complexation of choline chloride-ethylene glycol. *J Electroanal Chem*, 897 (2021) 115581.
- 32 Raste MN, Jagtap RM & Pardeshi SK, Optical second harmonic generation studies of pure and glycine-doped bithiourea copper/cadmium adipates. *J Mater Sci: Mater Electron*, 33 (2022) 10785.
- 33 Valarmathi S & Saravanan K, Growth and characterizations of pure and Cu-doped imidazolium L-tartrate (IMLT) single crystals: optical and NLO properties. *J Mater Sci: Mater Electron*, 33 (2022) 7573.
- 34 Imani MM, Kiani M, Rezaei F, Souri R & Safaei M, Optimized synthesis of novel hydroxyapatite/CuO/TiO<sub>2</sub> nanocomposite with high antibacterial activity against oral pathogen *Streptococcus mutans*. *Ceram Int*, (2021).
- 35 Pavithra M & Raj MBJ, Synthesis of ultrasonic assisted co-precipitated Ag/ZnO nanorods and their profound anti-liver cancer and antibacterial properties. *Mater Sci Eng B*, (2022) 115.
- 36 Hammud HH, McManus GJ, Zaworotko MJ, Tabesh RN, Ibrahim HIM, Ayub K & Ludwig R, The co-crystal of copper (II) phenanthroline chloride complex hydrate with p-aminobenzoic acid: structure, cytotoxicity, thermal analysis, and DFT calculation. *Monatsh Chem*, 152 (2021) 323.
- 37 Ivanova AD, Kuz'menko TA, Smolentsev AI, Sheludyakova LA, Klyushova LS, Bogomyakov AS, Lavrov AN & Lavrenova LG, Complexes of Copper(II) Halides with 2-(3,5-Dimethylpyrazol-1-yl) benzimidazole: Synthesis and Magnetic and Cytotoxic Properties. *Russ J Coord Chem*, 47 (2021) 751.
- 38 Eremina JA, Smirnova KS & Lider EV, Klyushova LS, Sheven' DG & Potkin VI, Nickel (II) and cobalt (II) complexes with 4,5-dichloro-isothiazole-3-carboxylic acid and 1,10-phenanthroline: synthesis, crystal structures and cytotoxicity. *Trans Met Chem*, 47 (2022) 19.